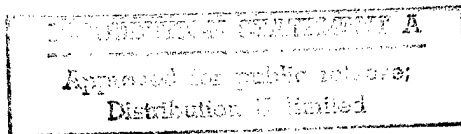# ⌀AIAA

AIAA 93-2660
STRAPDOWN STABILIZATION FOR IMAGING SEEKERS

Russell T. Rudin
Naval Air Warfare Center
Weapons Division
China Lake, CA

19980513 080

DTIC QUALITY INSPECTED 4

PLEASE RETURN TO:

BMD TECHNICAL INFORMATION CENTER
BALLISTIC MISSILE DEFENSE ORGANIZATION
7100 DEFENSE PENTAGON
WASHINGTON D.C. 20301-7100

2nd Annual
AIAA SDIO Interceptor Technology Conference
June 6-9, 1993 / Albuquerque, NM

U 46 26

Gov't Statement on page 1

Accession Number: 4626

Publication Date: Jun 06, 1993

Title: Strapdown Stabilization for Imaging Seekers

Personal Author: Rudin, R.T.

Corporate Author Or Publisher: U.S. Naval Air Warfare Center, China Lake, CA 93555-6011 Report
Number: AIAA 93-2660

Comments on Document: 2nd Annual AIAA SDIO Interceptor Technology Conference, June 6-9, 1993 at
Albuquerque, NM

Descriptors, Keywords: Stabilility Imaging Seeker Focal Plane Array FPA Sensor Acquisition Track
Discrimination Design

Pages: 00010

Cataloged Date: Aug 09, 1993

Document Type: HC

Number of Copies In Library: 000001

Record ID: 28017

Source of Document: AIAA

STRAPDOWN STABILIZATION FOR IMAGING SEEKERS

Russell T. Rudin
Naval Air Warfare Center Weapons Division
China Lake, CA 93555-6001 (Code C2944)

Approved for public release; distribution unlimited.

Abstract

In space constrained applications such as tactical missiles, locating the inertial sensors off the platform simplifies packaging and may allow existing missile autopilot gyros to be used for platform stabilization. In strapdown stabilization, inertial sensors are fixed to the base of the inertial platform rather than directly on the platform itself. Gimbal position sensor information is combined with body-fixed inertial rate sensor information to estimate the inertial rate of the platform. This estimate of platform rate is a key factor that determines the stabilization performance of the system.

An initial assessment of the feasibility of strapdown stabilization for high-resolution imaging seekers was conducted. A linear state space model and a detailed nonlinear planar simulation were developed of a tactical high-resolution platform system. The simulation includes gimbal inertia, inertial sensors, position sensors, friction, mechanical alignment, compliances, and control loop compensation. The simulation was used to predict the platform stabilization performance. In addition, effects of stabilization performance on target signal strength for an imaging seeker were estimated.

Nomenclature

ω_{pcmd}	Platform Inertial Rate Command
ε_{rl}	Platform Rate Error
T_{cmd}	Platform Torque Command
D/A	Digital-to-Analog Converter
A/D	Analog-to-Digital Converter
T_d	Disturbance Torque
T_{net}	Net Torque Applied to Platform
ω_p	Platform Inertial Angular Velocity
$\hat{\omega}_p$	Platform Inertial Angular Velocity Estimate or Measurement
λ	Gimbal Angle
$\dot{\lambda}$	Gimbal Rate
$\hat{\dot{\lambda}}$	Gimbal Rate Estimate
ω_m	Missile Body Inertial Angular Velocity
$\hat{\omega}_m$	Missile Body Inertial Angular Velocity Estimate or Measurement
N	Sensor Noise Input
J	Gimbal Moment of Inertia
A	System Matrix
B	Input Matrix
C	Output Matrix
x	State Vector
y	Output Vector
C_1, C_2	Rate Loop Compensator States
IS_1, IS_2	Inertial Sensor States
PS_1, PS_2, PS_3	Position Sensor States
D_1	Differentiator State
FOV	Field of View
IFOV	Instantaneous Field of View
FOG	Fiber Optic Gyro
QRS	Quartz Rate Sensor

Background

Imaging seekers usually consist of a focal plane array (FPA) sensor and optical system mounted to an inertial platform. The stabilization performance and subsequent image smearing of the platform in the presence of base motion is an important factor in determining acquisition and tracking performance. Shown in Figure 1 is a seeker that uses conventional stabilization. In the conventional seeker, the platform-mounted rate sensor feeds directly back to the gimbal torquer to provide stabilization. Base motion usually consists of missile rigid body motion, body bending, and often severe angular vibrations imparted from the launch platform. These input motions couple to the inertial platform via friction, wire compliance, cooling line compliance, and other coupling mechanisms. In addition, mass imbalance of the platform causes disturbances to the platform during missile body accelerations.
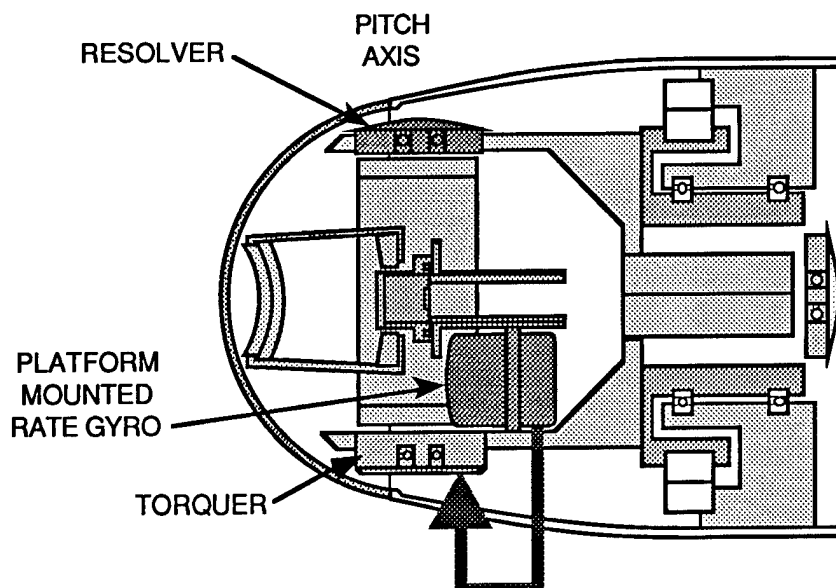
4624

Fig. 1. Conventional Rate Stabilized Platform.

"Platform stabilization" is defined as the undesirable inertial motion of the platform attributable to disturbances. The amount of platform stabilization required for a given imaging system depends primarily on the instantaneous field of view (IFOV), the system frame time, and the FPA integration time. "Image stabilization" is defined as the degradation of the image at the FPA attributable to platform stabilization. These two terms are defined because a given level of platform stabilization is not satisfactory to determine the suitability of strapdown stabilization. One must examine the optical system IFOV and FPA integration time. In this paper, platform stabilization is determined using a linear state space model and a nonlinear simulation for a strapdown stabilized seeker. The platform stabilization performance is then applied to a defined optical and FPA system to determine the image stabilization.

One of the key parameters of a strapdown stabilized seeker is the inertial rate sensor. This sensor usually determines the level of platform stabilization achievable for a given gimbal set. In this report, a low-cost inertial rate sensor, quartz rate sensor (QRS) and a higher-cost higher-performance fiber-optic gyro (FOG) were analyzed. Results for both sensors are presented.

An example of a remotely stabilized seeker is shown in Figure 2. Note that the output of the gyro is combined with that of the resolver to form the torquer feedback signal.

Baseline System Model

Shown in Figure 3 is the topology used for the baseline strapdown stabilization system. A tracker is assumed to provide inertial platform rate commands to the strapdown stabilization rate loop. The rate loop consists of compensation, gimbal inertia, position sensor, differentiator, and inertial rate sensor. The compensation transfer function is such that the resulting rate loop is type II. The position sensor used is a resolver combined with a resolver-to-digital (R/D) converter. The gyro is either a QRS or a FOG.

Note that missile body motion is essentially a disturbance input to the rate loop. The dynamics for the various components are shown below.

compensation: $\dfrac{700(s/50 + 1)}{s(s/1000 + 1)}$ when using QRS

$\dfrac{14092(s/300 + 1)}{s(s/3000 + 1)}$ when using FOG

Inertia: $J = 0.05$ oz-in-s^2

R/D Converter:
$$\dfrac{(s/7854 + 1)}{(s/18850 + 1)(s^2/3.578e8 + s/13398 + 1)}$$

2

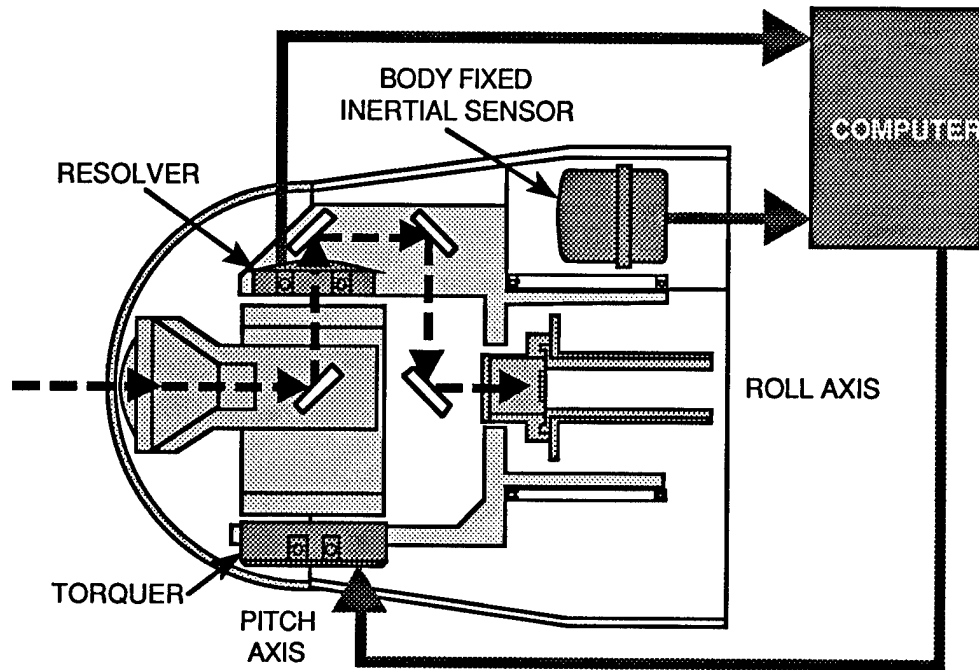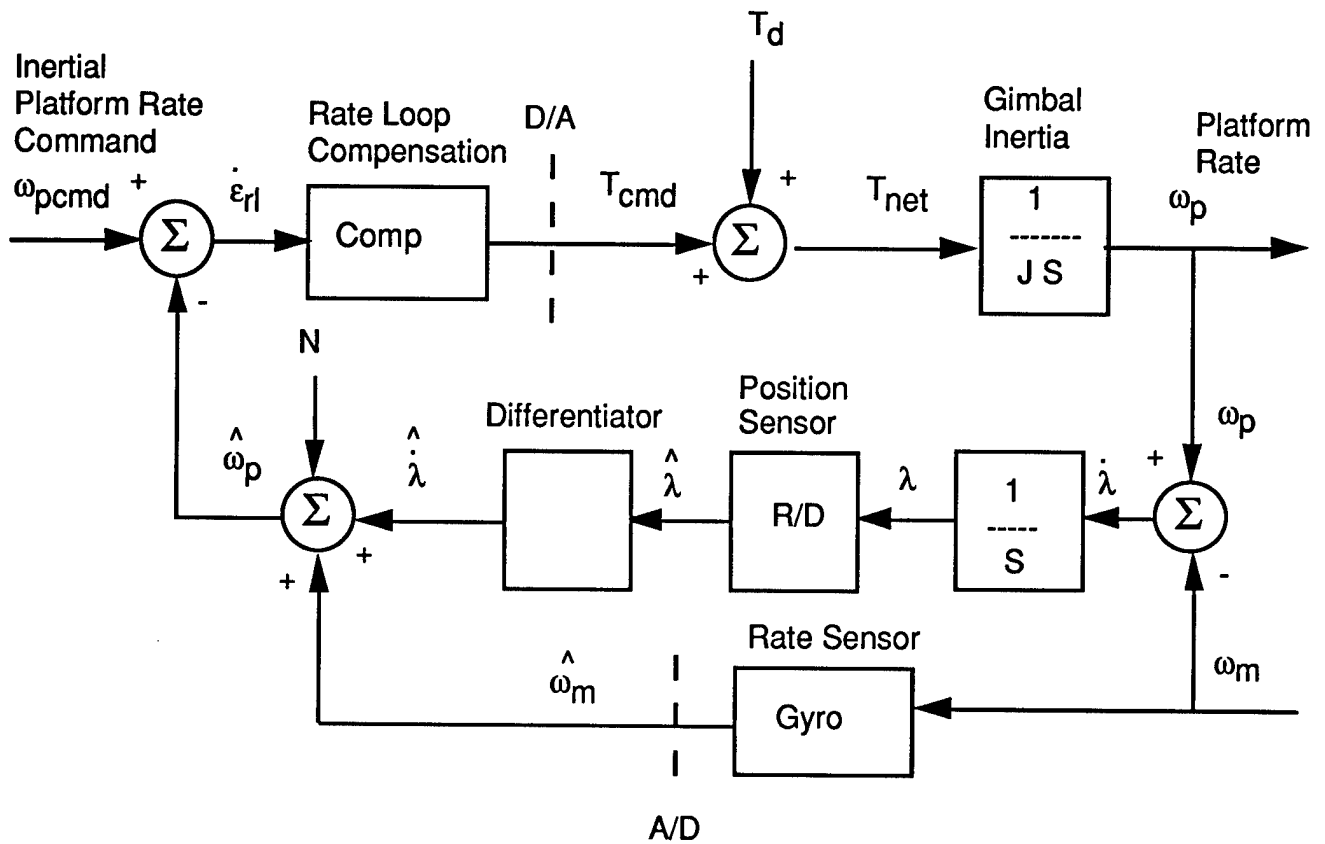Fig. 2. Strapdown Stabilized Seeker Concept.

Fig. 3. Baseline Strapdown Stabilization System.

Differentiator: $\dfrac{s}{(s/7560+1)}$

Gyro: QRS $= \dfrac{1.0}{(s^2/1.9455e5 + s/315.46 + 1)}$

FOG $= \dfrac{1.0}{(s/8820+1)}$

A state space representation of this model was developed and used to predict the platform stabilization attributable to disturbance torques and missile body motion. The maximum rate loop bandwidth for the QRS was limited by the power dissipation attributable to sensor noise. The QRS noise limits the bandwidth to 46 Hz, while the FOG rate loop bandwidth was chosen to be 150 Hz.

Linear State Space Model

A linear state space model was developed that includes the dynamics of the gyro, position sensor, differentiator, and control loop compensation. The three inputs are platform rate command, missile body motion, and disturbance torques. Outputs include platform inertial rate, platform inertial rate estimate, gyro output, gimbal rate estimate, and platform torque. Using the topology of Figure 3, a state space model of the strapdown stabilization rate loop was formed.

Using the notation for a linear time invariant system,

$\dot{x} = Ax + Bu$

$y = Cx$

The state vector "x" is defined as

$x = [C_1 \ C_2 \ \omega_p \ IS_1 \ IS_2 \ \lambda \ PS_1 \ PS_2 \ PS_3 \ D_1]^T$

The system inputs "u" are defined as

$u = [\ \omega_{pcmd} \ \omega_m \ T_d]^T$

The system outputs "y" are defined as

$y = [\omega_p \ \hat{\omega}_p \ \hat{\omega}_m \ \hat{\lambda}]^T$

This model was used to explore some of the input/output relationships of strapdown stabilization.

QRS Rate Loop

Using the QRS as the rate sensor and the state space representation defined above, a frequency response of the platform motion attributable to missile motion, $\omega_p(s)/\omega_m(s)$, was obtained and is shown in Figure 4.

Notice that as the frequency of missile body motion increases, platform motion increases until reaching the rate loop bandwidth at which point the rate loop provides no stabilization. The cause of this missile body coupling can be understood by taking the baseline rate loop and simplifying it as shown in Figure 5. In this figure, the disturbance torque and rate command inputs have been omitted.

In Figure 5 the gyro is designated G1; the physical integrator, R/D converter, and the differentiator are designated G2; and the gimbal moment of inertia and rate loop compensation are designated H. Using block-diagram-reduction techniques, a transfer function for platform rate estimate attributable to missile body motion can be found.

$$\frac{\hat{\omega}_p(s)}{\omega_m(s)} = \left[\frac{G1}{G2} - 1\right]\left[\frac{G2}{1 - G2\,H}\right]$$

The difference in dynamics of the gyro (G1) and the R/D converter/differentiator (G2) causes the missile body motion coupling. Thus, if the dynamics of the gyro and R/D converter/differentiator were identical, body coupling will not exist. Since, in general, the dynamics of the R/D are faster than the gyro, the easiest approach is to filter the R/D/differentiator to match the low-frequency dynamics of the gyro. Another approach is to increase the bandwidth of the gyro via compensation to match the dynamics of the R/D converter/differentiator. This approach tends to amplify inertial sensor noise. A third approach is to pick some intermediate dynamics that have a bandwidth between the gyro and R/D/differentiator and modify the dynamics of both to match the selected intermediate value.

A first attempt at matching the dynamics of the two sensors consists of filtering the R/D converter output with the transfer function of the gyro. Minor modification to the rate loop compensation was required to ensure adequate phase margin. The response of this modified system to missile body motion is shown in Figure 6. Note that platform motion has been reduced by almost 20 dB compared to Figure 4, which does not have the matched dynamics between gyro and R/D converter. The suitability of this level of stabilization performance will be discussed in the simulation section of this paper.
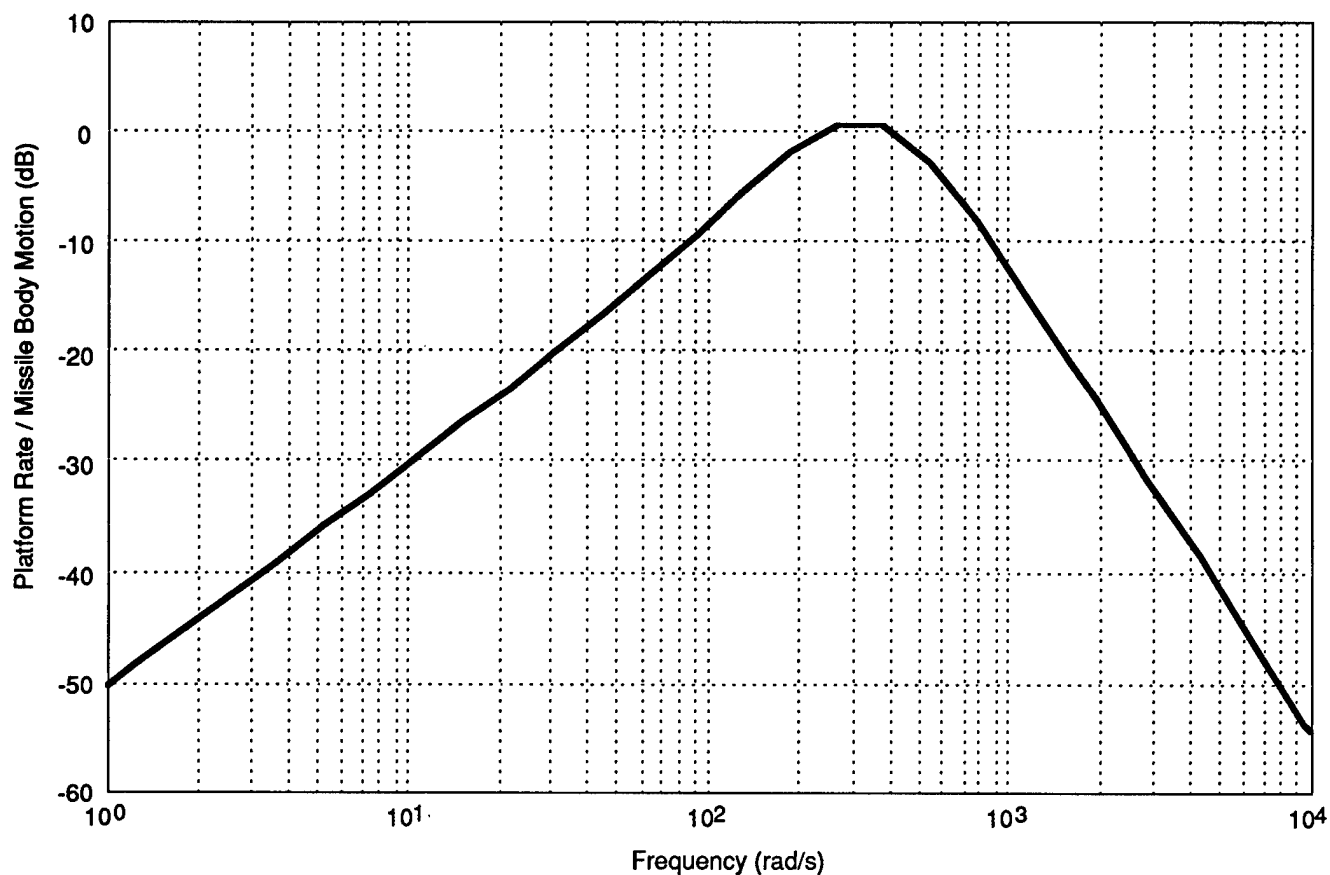
4

Fig. 4. Platform Motion Resulting From Missile Motion [$\omega_p(s)/\omega_m(s)$] Using QRS With 46 Hz Bandwidth Rate Loop.
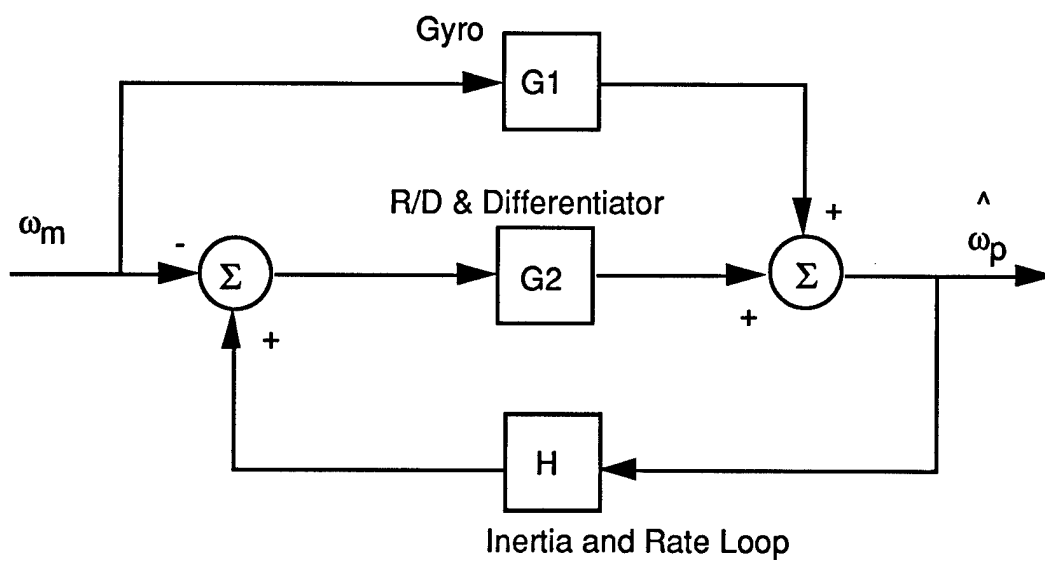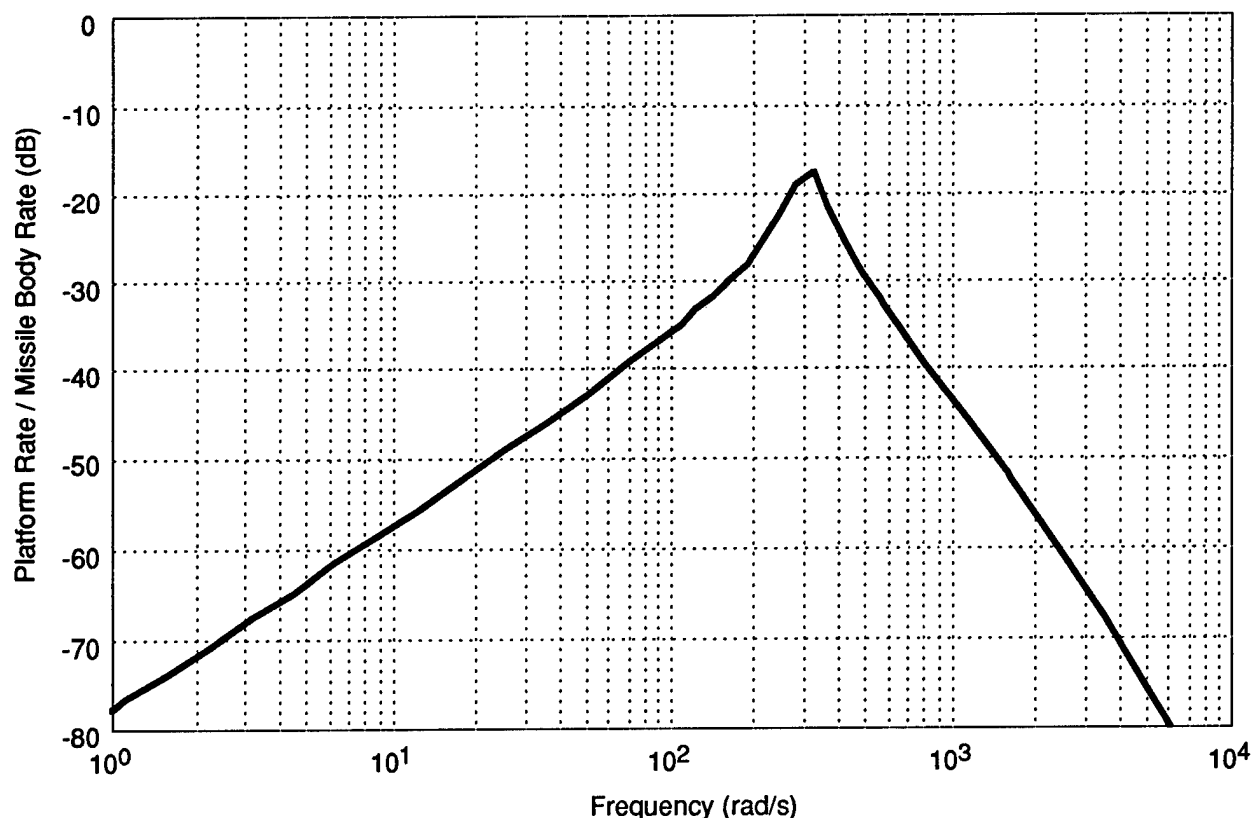

Fig. 5. Simplified Rate Loop.

5

Fig. 6. Platform Motion Resulting From Body Motion Using Matched Dynamics.

FOG Rate Loop

The FOG is a high-performance inertial angular rate sensor. Its high bandwidth, low noise, and low bias make it a desirable sensor for remote stabilization. A rate loop bandwidth of 150 Hz was selected for the FOG. A state space model of the rate loop using the FOG was developed using the same form as for the QRS. The platform rate attributable to missile body motion $(\omega_p(s)/\omega_m(s))$ is shown in Figure 7.

Notice the significantly reduced platform motion when compared to the QRS performance shown in Figure 6. Dynamic matching of the low-frequency dynamics of the gyro and R/D converter/differentiator is not required with the FOG. The low-frequency dynamics are close enough without dynamic matching. The suitability of this stabilization performance will be discussed in the simulation section of this report.

Platform Simulation

A detailed non-linear single-axis simulation of a strapdown stabilized seeker was developed and tested. This simulation includes

1. 3-Hz bandwidth digital tracking loop dynamics

2. 46- or 150-Hz bandwidth digital rate loop dynamics for the QRS and FOG, respectively.
3. Quantization
4. D/A and A/D conversions
5. Gimbal coulomb friction
6. Gimbal inertia
7. Rate sensor dynamics and error sources (QRS and FOG)
8. Position sensor dynamics and error sources
9. Platform rate estimation algorithms
10. Gimbal to sensor misalignment

The simulation has inputs for target and missile body motion. For evaluating strapdown stabilization performance, a target with zero line-of-sight (LOS) rate is tracked. The missile body is then moved at various rates and frequencies to see the resulting platform motion. The missile body is moved through sinusoidal motions that are representative of free flight and captive carry. In free flight, airframe rigid body motion is low frequency and high amplitude. The captive carry environment is characterized by high-frequency low-amplitude body rates. The captive carry environment is also similar to the body bending experienced during free flight. Simulation runs were performed for three free flight environments and one captive carry environment as shown in Table 1.
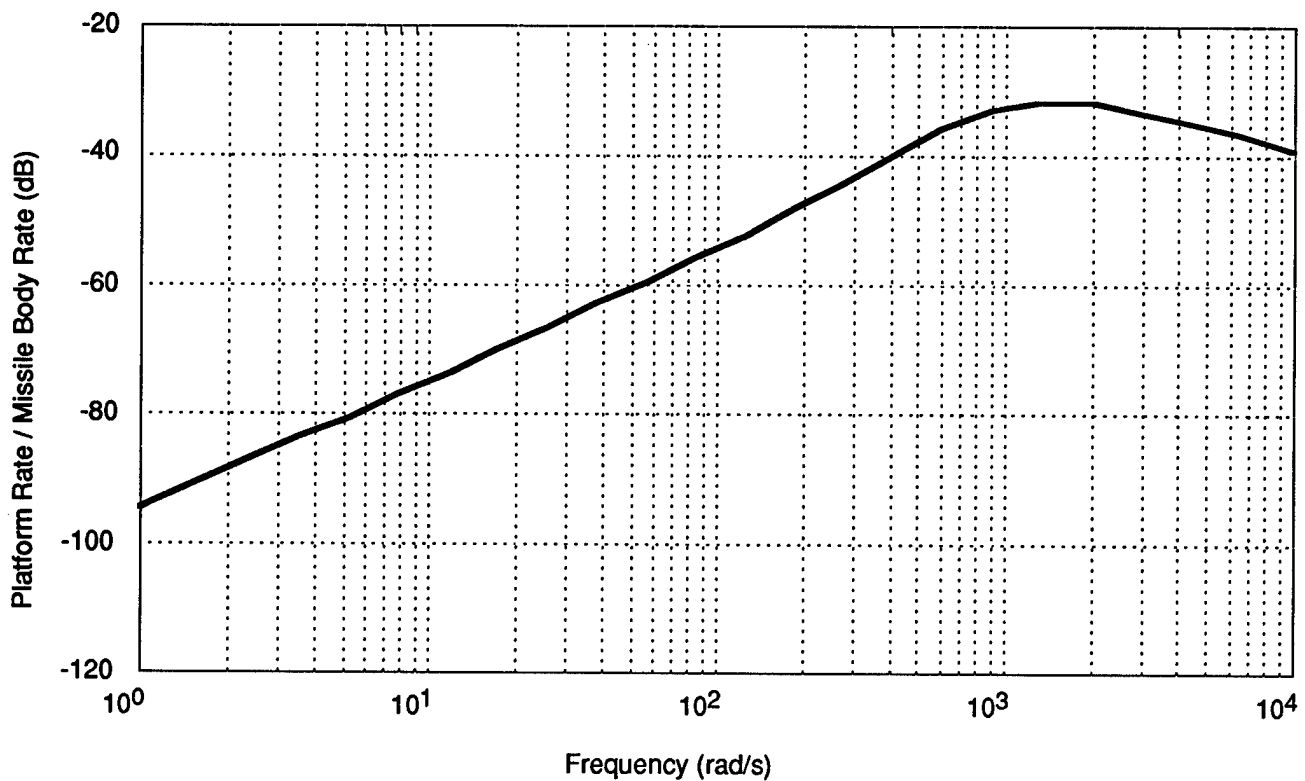
6

Fig. 7. Platform Motion Resulting From Missile Body Motion Using FOG With 150 Hz Rate Loop.

Table 1. Missile Body Input Rate for Simulation.

Environment	Rate - ω_m	
	deg/s	Hz
Free flight no. 1	130	5
Free flight no. 2	260	2.5
Free flight no. 3	430	5
Captive carry	315	50

These body inputs were run for both the QRS and FOG rate loops. Time histories were obtained for platform rate and track error. Shown in Figure 8 is the platform rate for the QRS rate loop attributable to free flight environment no. 1.

The track error for the same simulation run is shown in Figure 9. In this figure, the platform motion coincides with the missile body motion.

These data show the stabilization performance of the rate loop using the QRS sensor. As mentioned previously, the stabilization performance data of the platform are not sufficient to determine the suitability for an imaging system. One must also consider the optical resolution and integration time of the FPA.

Image Stabilization Program

Once platform stabilization data have been obtained, the effect on image stabilization can then be determined.

Image stabilization depends primarily on the system optical resolution and the FPA integration time. When considering the detection and tracking of single pixel targets, the amount of energy that spills over into adjacent pixels as a result of platform motion is a significant issue. Everything else being equal, the longer the integration time, the better the stabilization performance required. Similarly, high-resolution systems require better platform stabilization to maintain small targets on a single pixel.

A computer program was written that estimates the loss of signal strength on the FPA attributable to platform stabilization. This Image Stabilization Program (ISP) simulates the projection of an image with unity intensity onto an FPA. The ISP inputs platform motion data from the platform simulation and calculates the resulting signal strength attributable to platform stabilization. Because it has been normalized, the resulting signal strength will be somewhere between zero and one. The ISP can be set for different optical resolutions (IFOV), integration times, frames times, and target sizes. A graphical output shows a three-dimensional picture of the image for each frame and the signal strength for the strongest pixel. Shown in Figures 10 and 11 are a representative output of the ISP. For these figures a system IFOV of 0.5 mrad, FPA integration time of 1 millisecond, and a frame time of 12.5 milliseconds was assumed.
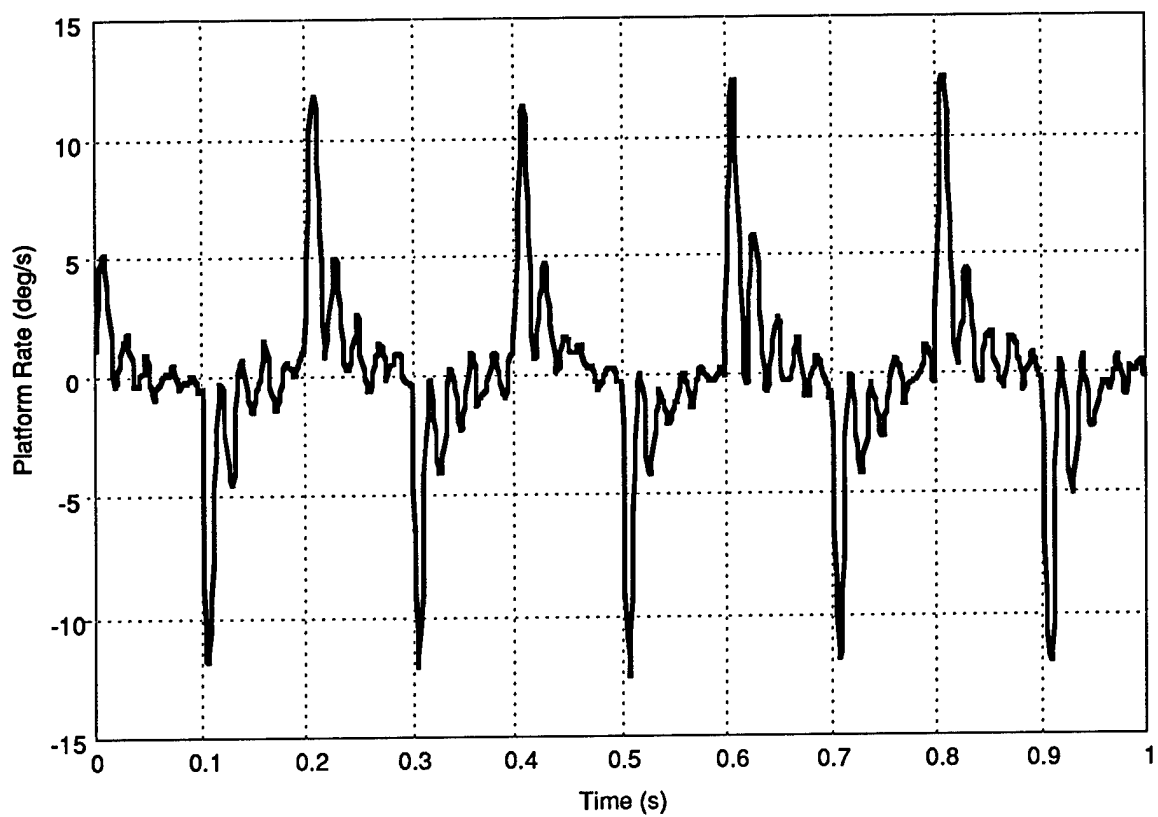
7

Fig. 8. Platform Rate as a Result of Body Motion Using QRS Rate Loop, Free Flight No. 1.
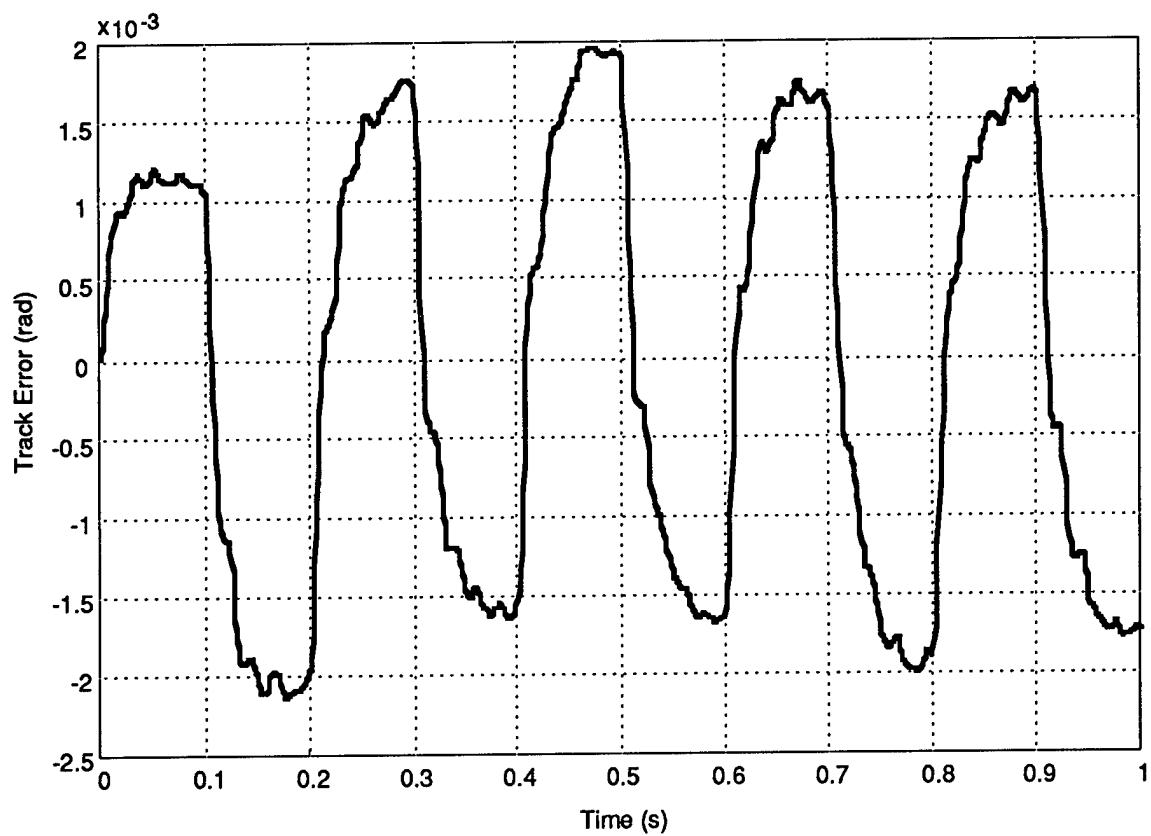

Fig. 9. Track Error as a Result of Body Motion Using QRS Rate Loop, Free Flight No. 1.
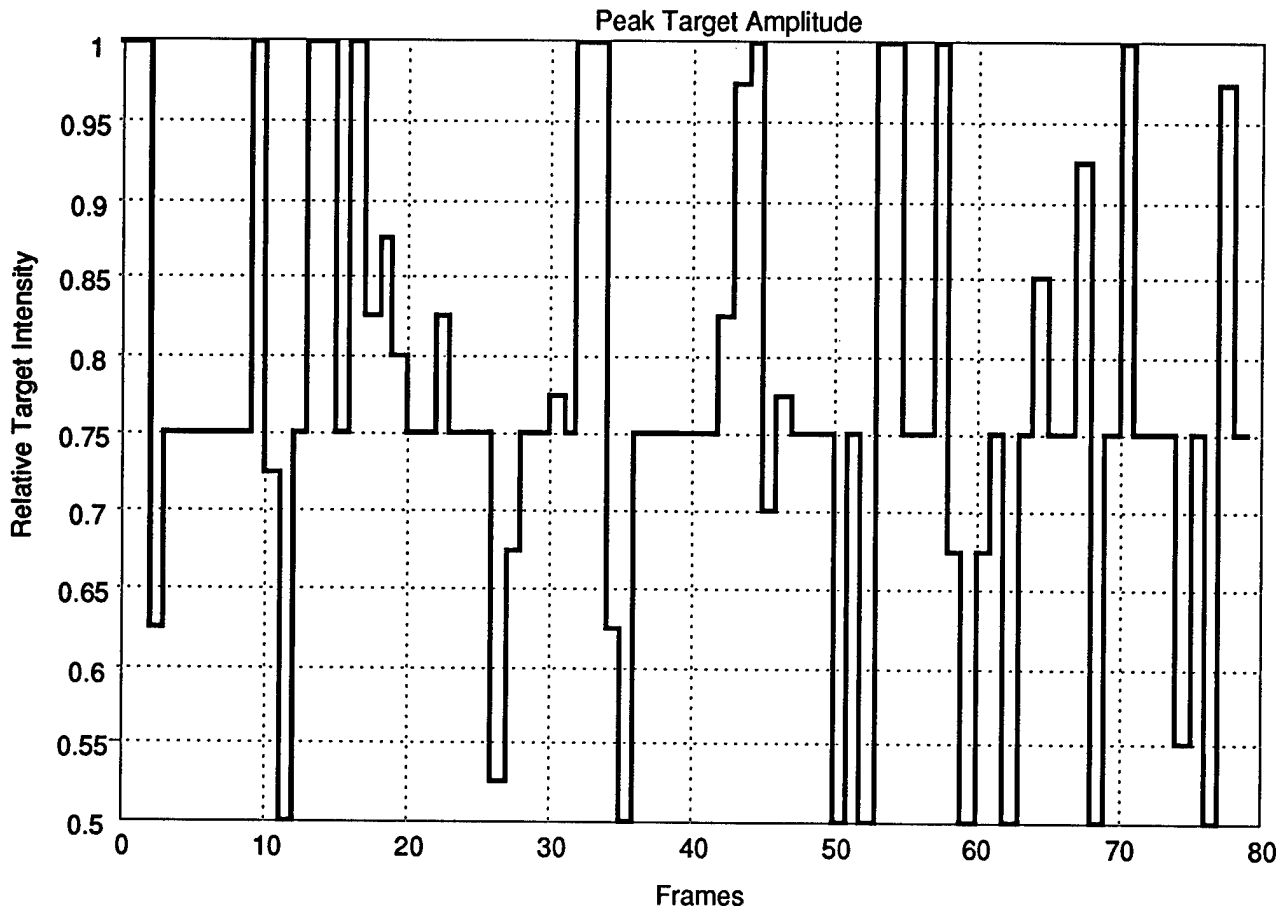
Fig. 10. Normalized Peak Amplitude as a Result of Body Motion Using QRS Rate Loop, Free Flight No. 1.

Figure 10 shows the peak amplitude of the signal for each frame attributable to platform stabilization. Ideally, the amplitude of each frame should be unity indicating that the platform motion does not degrade the signal strength.

Figure 11 shows a representative 3-D intensity plot for a single frame. Each square represents one pixel. The signal falling on the FPA is 3x3 pixels with unity amplitude. The figure shows the loss of signal attributable to platform motion.

A series of runs were performed using data from the platform simulation. Shown in Tables 2 and 3 are the platform stabilization levels and the mean and standard deviation of the peak signal strength obtained from both the QRS and FOG rate loops.

Note that the platform stabilization of the FOG is much better than the QRS. However, differences in the mean peak signal strength between the two rate sensors are less than 15%. The relatively short integration time of the FPA (1 millisecond) is the reason for this small difference. Thus, the additional stabilization performance of the FOG has a marginal effect on peak signal strength. Of course, many other factors must be considered in selecting the appropriate amount of platform stabilization and related rate sensors. This analysis has only considered signal strength and not other important factors such as the effect of false target motion on image processing algorithms.
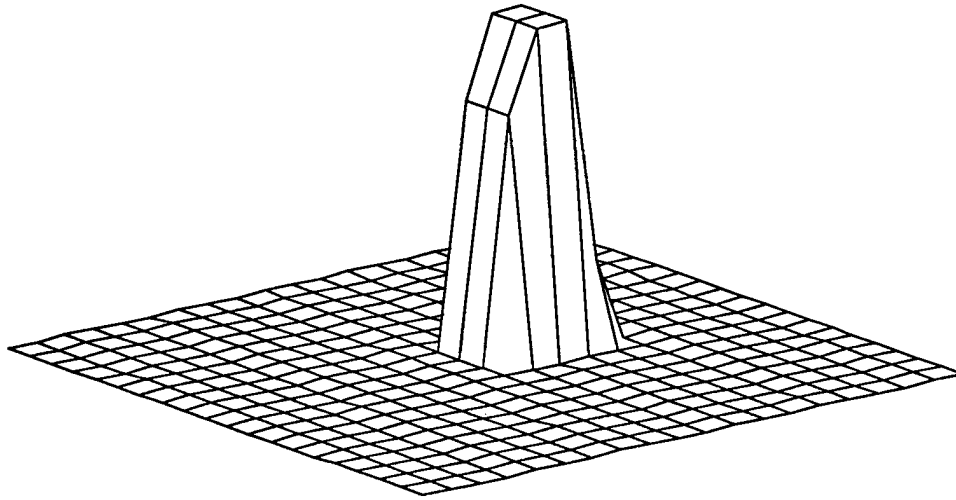
Fig. 11. 3D Plot of Signal Intensity.

Table 2. Platform Stabilization and Peak Signal Amplitude Using QRS.

Environment	Platform stabilization	Normalized peak signal amplitude			
		1-pixel-area target		4-pixel-area target	
Body motion	1 σ platform motion, mrad	Mean	1 σ	Mean	1 σ
Free flight no. 1	1.4	0.77	0.14	1.0	0.0
Free flight no. 2	2.0	0.75	0.19	1.0	0.0
Free flight no. 3	1.4	0.75	0.18	1.0	0.0
Captive carry	1.2	0.74	0.12	0.98	0.03

Table 3. Platform Stabilization and Peak Signal Amplitude Using FOG.

Environment	Platform stabilization	Normalized peak signal amplitude			
		1-pixel-area target		4-pixel-area target	
Body motion	1 σ platform motion, mrad	Mean	1 σ	Mean	1 σ
Free flight no. 1	0.05	0.94	0.10	1.0	0.0
Free flight no. 2	0.08	0.85	0.12	1.0	0.0
Free flight no. 3	0.08	0.88	0.12	1.0	0.0
Captive carry	0.06	0.86	0.12	1.0	0.0

Summary

The use of strapdown stabilization for high-resolution imaging systems has been assessed for the missile body motion inputs using analysis and simulation of a single-axis gimbal system. Realistic system parameters were used to simulate the gimbal and its control loop compensation. Factors such as gimbal friction, gimbal alignment, quantization, discrete-time algorithms, and sensor dynamics were included in the simulation.

Using the QRS, the 1-σ stabilization performance ranged from 1.2 to 2.0 milliradians. When this level of platform stabilization is applied to an imaging seeker with 0.5-milliradian IFOV and 1-millisecond FPA integration time, the normalized mean peak signal strength was about 0.75 with a standard deviation of about 0.18.

The FOG was able to achieve a 1-σ stabilization performance of 0.05- to 0.08-milliradian, or about 15 times better than the QRS. However, the normalized mean peak signal strength increased only marginally: 0.85 to 0.94 with a standard deviation of 0.12. Thus, the additional stabilization performance of the FOG has a marginal effect on signal strength in this case.

The technique of matching the low-frequency dynamics of the sensors reduces the missile body coupling to acceptable levels. The stabilization performance obtained in this study is consistent with that required for imaging seekers. To further explore the area of strapdown stabilization, a 3-degree of freedom gimbal simulation should be developed that would allow missile body motion to be input in three axes.